Atmos. Chem. Phys. Discuss., 9, 20913–20948, 2009
www.atmos-chem-phys-discuss.net/9/20913/2009/

Atmospheric
Chemistry
and Physics
Discussions

Circumpolar measurements of speciated mercury, ozone and carbon monoxide in the boundary layer of the Arctic Ocean

J. Sommar[1], M. E. Andersson[2], and H.-W. Jacobi[3,4]

[1]State key Laboratory of Environmental Geochemistry, Institute of Geochemistry, Chinese Academy of Sciences, Guiyang 550002, China
[2]Department of Chemistry, Göteborg University, 41296 Göteborg, Sweden
[3]Laboratoire de Glaciologie et Géophysique de l'Environnement, CNRS – Université Joseph Fourier Grenoble, 54 Rue Molière, 38400 St Martin d'Hères, France
[4]Alfred Wegener Institute for Polar and Marine Research, Am Handelshafen 12, 27570 Bremerhaven, Germany

Received: 19 August 2009 – Accepted: 20 August 2009 – Published: 5 October 2009

Correspondence to: J. Sommar (jonas@mails.gyig.ac.cn)

Published by Copernicus Publications on behalf of the European Geosciences Union.

Abstract

Using the Swedish icebreaker Oden as a platform, continuous measurements of airborne mercury (gaseous elemental mercury (Hg^0), divalent mercury Hg^{II}(g) (acronym RGM) and mercury attached to particles (PHg)) and some long-lived trace gases (carbon monoxide CO and ozone O_3) were performed over the North Atlantic and the Arctic Ocean. The measurements were performed for nearly three months (July–September, 2005) during the Beringia 2005 expedition (from Göteborg, Sweden via the proper Northwest Passage to the Beringia region Alaska – Chukchi Penninsula – Wrangel Island and in-turn via a north-polar transect to Longyearbyen, Spitsbergen). The Beringia 2005 expedition was the first time that these species have been measured during summer over the Arctic Ocean going from 60° to 90° N.

During the North Atlantic transect, concentration levels of Hg^0, CO and O_3 were measured comparable to typical levels for the ambient mid-hemispheric average. However, a rapid increase of Hg^0 in air and surface water was observed when entering the ice-covered waters of the Canadian Arctic archipelago. Large parts of the measured waters were supersaturated with respect to Hg^0, reflecting a strong disequilibrium. Heading through the sea ice of the Arctic Ocean, a fraction of the strong Hg^0 pulse in the water was spilled with some time-delay into the air samples collected ~20 m a.s.l. Several episodes of elevated Hg^0(g) were encountered along the sea ice route with higher mean concentration (1.81±0.43 ng m^{-3}) compared to the marine boundary layer over ice-free oceanic waters (1.55±0.21 ng m^{-3}). In addition, an overall majority of the variance in the temporal series of Hg^0 concentrations was observed during July. Atmospheric boundary layer O_3 mixing ratios decreased when initially sailing northward. In the Arctic, an O_3 minimum around 15–20 ppbv was observed during summer (July–August). Alongside the polar transect during the beginning of autumn, a steady trend of increasing O_3 mixing ratios was measured returning to initial levels of the expedition (>30 ppbv). Ambient CO was fairly stable (84±12 ppbv) during the expedition. However, from the Beaufort Sea and moving onwards steadily increasing CO mixing ratios were observed (0.3 ppbv day^{-1}). On a comparison with coeval archived CO and O_3 data from the Arctic coastal strip monitoring sites Barrow and Alert, the observations from Oden indicate these species to be homogeneously distributed over the Arctic Ocean. Neither correlated low ozone and GEM events nor elevated concentrations of RGM and PHg were at any extent sampled, suggesting that atmospheric mercury deposition to the Arctic basin is low during the Polar summer and autumn. Elevated levels of Hg^0 and CO were episodically observed in air along the Chukchi Peninsula indicating transport of regional pollution.

1 Introduction

The average residence time of gaseous elemental mercury (Hg^0) and carbon monoxide (CO) in the lower troposphere is sufficient to make its distribution homogeneous over each hemisphere. While the seasonal cycle of CO exhibits a summertime minimum largely due to chemical oxidation initiated by the hydroxyl radical OH (e.g. Holloway et al., 2000), the seasonality of Hg^0 is less obvious taking into consideration worldwide long-term observations (Kim et al., 2005). However, several background stations in the mid-latitudes north of 45° N (Kellerhals et al., 2003; Kim et al., 2005) and in the Southern Hemisphere (Slemr et al., 2008) report a wintertime Hg^0 maximum. This has been attributed to seasonal trends in anthropogenic emissions and/or meteorological conditions, atmospheric oxidation processes, the altitude of the atmospheric mixing layer (Kock et al., 2005) and the terrestrial carbon pool (Obrist, 2007). Unlike Hg^0 and CO, the mixing ratio of ozone (O_3) in the lower troposphere reaches a maximum during summer. The Arctic atmospheric boundary layer Hg^0 and O_3 cycles derived from background observation sites in the European and American high Arctic (Schroeder et al., 1998; Berg et al., 2003; Helmig et al., 2007), however, exhibit large seasonal discrepancies from that of the mid-latitudes.

It has been elucidated that high levels of neurotoxic mercury in the Arctic ecosystems is partially linked to rapid, near-complete depletion of Hg^0 (MDEs) in the atmospheric boundary layer occurring episodically during the polar spring (Steffen et al., 2008). Upon reaction with reactive bromine species such as bromine atoms (Donohoue et al., 2006) hundred(s) of tons of oxidised mercury (Hg^{II}) are produced and perennially deposited into the Arctic environment (Ariya et al., 2004; Banic et al., 2003; Dastoor et al., 2008; Skov et al., 2004). The relative magnitude of this sink is huge, resembling almost half of the annual atmospheric input within a few weeks (Outridge et al., 2008). To a yet not well quantified, but significant degree, a back-reduction of Hg^{II} to Hg^0 occurs resulting in a re-cycling of volatile mercury to the atmosphere (Schroeder et al., 2003). However, it cannot compensate for the total deposition, and a net assimilation into the food chain occurs. The Hg levels in the traditional food of indigenous people living in the Arctic pose a threat for human pre- and neonatal neurological development (Steffen et al., 2008). Arctic marine mammals such as beluga whales frequently contain total Hg levels well above Canadian Federal Consumption Guidelines (Lockhart et al., 2005). Again, the fate of surplus mercury deposited to the Arctic basin during polar spring is largely indefinite with reference to transport and transformation. This issue has recently been discussed in modelling papers by Hedgecock et al. (2008) and Outridge et al. (2008) in favour of less net accumulation in the abiotic reservoirs. The Beringia 2005 expedition, taking place a few months after the period of elevated deposition of Hg to the Arctic Ocean, offered a unique opportunity to sample vast exposed, yet unexplored areas.

During the polar spring MDEs, Hg^0 is generally strongly correlated with O_3 (e.g. Ebinghaus et al., 2002; Eneroth et al., 2007). The loss of tropospheric O_3 and most probably Hg^0 in the Arctic is initiated by catalytic heterogeneous reactions involving reactive bromine gases that originate from refined sea salt reservoirs linked to sea ice; e.g. frost flowers (Kaleschke et al., 2004; Jacobi et al., 2006) or snow on sea ice (Simpson et al., 2005) and is activated by gas-phase photochemistry: Young ice regions with open leads tend to promote the growth of salinity-enhanced ice crystals with large effective surface areas. Hönninger (2002), Brooks et al. (2006) and Sommar et al. (2007) reported ground-based measurement of elevated BrO concentration in concert with air masses depleted of Hg^0 and O_3. Unlike Hg^0(g) and O_3(g), CO(g) is less susceptible to bromine radical initiated degradation and hence essentially remaining chemical inert during polar spring (Sumner et al., 2002). The spatial extent of MDEs may be approximated using satellite observations of BrO and ground-based observations (Garbarino et al., 2002; Hollwedel et al., 2004; Lahoutifard et al., 2006; Poulain et al., 2007b; Simpson et al., 2005). During the rest of the year the atmospheric reactions driving the cycling of Hg in the boundary layer is ambiguous, possibly involving HO_x and NO_y radicals (Calvert and Lindberg, 2005; Sommar et al., 2001; Sommar et al., 1997). Therefore, it is important to co-sample Hg^0(g) with other long-lived atmospheric species. Recently, the Hg/CO emission ratio from long-distance transported pollution episodes to remote observation sites has been employed to estimate the anthropogenic Hg^0 emissions from eastern Asia (Jaffe et al., 2005) and Europe (Slemr et al., 2006) as well as emissions from large scale forest fires (Ebinghaus et al., 2007; Sigler et al., 2003). Selected studies suggest a substantial underestimation of source strength of Hg^0 in the current inventories for East Asia and Europe, respectively. We have already pointed out that the regimes of O_3 are similar with that of Hg^0 during MDEs, in addition it is produced from degradation of CO by OH radicals, so O_3 is an eligible candidate.

A main objective was to estimate the spread of mercury in the Arctic environment and to investigate the lability of the deposited Hg^{II} compounds in condensed phases with respect to reduction. During the polar transect of the Arctic Ocean from Alaska to Spitsbergen, speciated Hg-measurements were performed including gaseous divalent Hg species (RGM) and Hg attached to fine particles (PHg) in addition to that of Hg^0(g), O_3(g) and CO(g). PHg has turned out to be a regional tracer for combustion in Europe (Wängberg et al., 2003). This paper focuses on the air measurements alone and is a companion paper of those dealing with mercury in sea water (surface and deep-sea), ice, snow, and sediments collected in the Arctic Ocean (Andersson et al., 2008b and Andersson, in preparation).

2 Experimental

2.1 Sampling location

The measurements were conducted on board the icebreaker Oden. The IB Oden is a 108 m long and 31 m wide icebreaker, which has been rebuild to meet scientific demands. The ship is equipped with meteorological and oceanographic instrumentation. The cruise (track outlined in Fig. 1) was divided into three legs: 1. Göteborg, Sweden – Barrow, Alaska, 2. Barrow – Chukchi Peninsula – Barrow, 3. Barrow – Longyearbyen, Spitsbergen. Ambient air samples were continuously collected and analysed using automatic instruments. The instruments were housed in a heated container laboratory at the 4th deck fronting the stem (~20 m a.s.l.). Further information is summarised in Table 1.

2.2 Mercury measurements

A Tekran® (Model 2537A) gas-phase mercury vapour analyser instrument was used to measure total gaseous mercury (TGM). TGM refers to gaseous elemental mercury (Hg^0) and small contributions of other gaseous mercury species (<1% at ambient conditions) that may pass through the sampling line and be detected as Hg^0 (Temme et al., 2003). The instrument utilised two gold cartridges in parallel, with alternating operation modes (sampling and desorbing/analysing in mercury free Ar stream) on a predefined time base of 5 min. A 0.45 µm Teflon filter protected the sampling cartridges against contamination by particulate matter. Ambient air was sampled with a flow rate of 1.5 L min^{-1}. The exposure to marine air tends to permanently passivate the gold cartridges. Therefore, the cartridges were changed frequently. To prevent deactivation the cartridges were ultrasonically cleaned in a Labosol® wash, repeatedly rinsed with Milli-Q water and dried in a mercury free stream of argon. The performance of the cartridges was routinely checked by injections from internal and external temperature controlled mercury sources. All concentrations are calculated to represent mass of Hg^0 per m^3 of air at STP (0°C and 1013 hPa). The method detection limit was $<0.15\,ng\,m^{-3}$ for a 5 min sample calculated as $1\times\sigma$.

During the 3rd leg of the Beringia 2005 expedition, an automatic set-up was used to simultaneously measure RGM and PHg (Wängberg et al., 2008). The air to be sampled was pulled through a specially designed intake consisting of a Teflon coated elutriator with an acceleration jet with 2.5 µm cut-off and then into a 20 cm long KCl coated annular quartz glass denuder (URG-2000-30 K and URG-2000-30CD, University Research Glass Corp, Chapel Hill, NC, USA). A filter holder (made from quartz glass) was placed vertically downstream the KCl denuder. Fine particles (≤2.5 µm) were collected on a quartz glass fibre filter of 20 mm diameter. The denuder and the particle filter were placed in separate ovens followed by a pyrolyser unit kept at 750°C. The apparatus was assembled in a temperature controlled aluminium box fixed to the gun whale. The sample intake was located in the bottom of the aluminium box ~20 m above sea level. The denuder was kept at 50°C during sampling to protect the KCl coating from humidity. During analysis both the denuder and quartz filter were purged with mercury-free air. During the initial step of the analysis the particle filter was heated to 600°C. PHg on the trap was desorbed and thermo-reduced to Hg^0 when passing the pyrolyser. In the next step, while the particle trap was maintained at high temperature, the denuder was heated to 540°C. At 500°C, RGM was desorbed from the KCl-matrix and totally decomposed to Hg^0 in the pyrolyser. The desorbed Hg^0 pulses were transferred via a thermally insulated FEP tubing temperature controlled at 60°C to the Tekran® instrument (described above) for mercury detection. RGM and PHg samples were collected with a flow rate of $8.5\,L\,min^{-1}$ during 5 h effective sampling time with an intervening period of 1 h for analysis. The method detection limit (MDL) of RGM and PHg were 3 and $1.5\,pg\,m^{-3}$, respectively, calculated as $1\times\sigma$.

In the following, no distinction will be made between the TGM and Hg^0(g) measurements performed. The acronym Hg^0/TGM used below is justified by comparing the precision of the Tekran instrument with the actual concentrations of RGM and PHg measured.

2.3 Ozone and carbon monoxide measurements

Surface level O_3 mixing ratios were measured continuously using a commercial analyser based on UV absorption ($O_3$41M, Ansyco GmbH, Karlsruhe, Germany). The same instrument has been used before during cruises on the Atlantic and Arctic Oceans (Jacobi and Schrems, 1999; Jacobi et al., 2006). It was operated with an integration time of 10 min. Calibrations were invoked on a daily basis using an internal ozone generator. The detection limit was 1 ppbv at a sampling rate of 1 L min^{-1}.

CO mixing ratios were determined also using a commercial detector employing a vacuum-UV resonance fluorescence technique (AL 5001, Aero-Laser GmbH, Garmisch-Partenkirchen, Germany). Details of the instrument can be found elsewhere (Gerbig et al., 1999). Air samples were collected with a time resolution of 0.5 min. The instrument was calibrated daily using a certified CO/synthetic air mixture from cylinders. For zero measurements, ambient air was used after removal of CO by oxidation with Pd-catalyst (150°C). The detection limit was <1 ppbv. The air inlet (FEP tubing, 10 m long) for both instruments was positioned in a protective housing (Savillex Corp.) in the top of a pylon located 3 m above the 4th deck (approximately 22 m a.s.l.).

2.4 Ancillary data

Meteorological and basic seawater parameters were measured by the ship's monitoring system. The air parameters were measured 30 m above the sea surface while the aquatic parameters were obtained from the bow-water intake located approximately 5 m beneath the sea surface.

Backward trajectories were calculated with the Hybrid Single-Particle Lagrangian Integrated Trajectory (HYSPLIT) Model (Draxler and Rolph, 2003). The calculations were made interactively using the FNL meteorological data sets. The stability of the back trajectories was verified by expanding the starting area fetch or by calculating at different starting heights. The 5-day back-trajectories were classified as of either 1) North Atlantic oceanic, 2) Canadian Arctic archipelago, 3) Arctic oceanic, 4) North

Pacific oceanic or 5) Chukchi Peninsula/Siberian origin (cf. Fig. 1).

Further data for 2005 regarding CO and O_3 measured at the arctic coastal stations Alert, Canada and Barrow, Alaska are also presented. CO data from Barrow were provided by Paul Novelli (NOAA/ESRL, personal communication, 2009). O_3 data at Alert were obtained within the Canadian Air and Precipitation Monitoring Network (CAPMoN) of the Air Quality Research Division of Environment Canada. Further data (O_3 at Barrow and CO at Alert) were retrieved from the WMO World Data Centre for Greenhouse Gases (gaw.kishou.go.jp/wdcgg.html). All data are available as 1 h averages.

2.5 Data analysis

The raw sampling data of Hg^0/TGM, CO and O_3 was averaged with a common time base of 10 min. The composite data points were further investigated for abnormal high and low concentrations. Using a ship as sampling platform, it is inevitable to avoid sampling the plume of the internal engine. It can be expected that in the combustion plume, which contains large amounts of nitrogen oxides, the ratio between O_3 and CO changes significantly due to the consumption of O_3 by the following reaction:

$$NO + O_3 \rightarrow NO_2 + O_2 \qquad \text{(R1)}$$

Since it is impractical to avoid episodically sampling the ship's plume, it is handy to screen the data by using the O_3/CO ratio. Mercury in crude oil is a catalyst's poison and has to be removed before processing the lighter fractions. However, the heavier fractions used for ship fuel may contain Hg in the ppb-range (Wilhelm, 2001). It is thus imperative to investigate and possibly screen the Hg^0 data to remove values influenced by emissions from the ship (Aspmo et al., 2006; Slemr et al., 1985). These rather frequent local pollution events exhibit an enhanced CO and low O_3 concentration. Exclusion of data points was therefore based on crossing a CO/O_3-limit with certain conditions of the two variables and/or by wind direction (see below). To be able to examine the diurnal variability, the data points were lumped into 1 h bins representing the local time instead of UTC. Statistical evaluation and conventional data plots were made using Plot-It (v. 3.2, Scientific Programming Enterprises, USA) as well as ProFit (v. 6.1.7, Quantum Soft, Switzerland) statistical software. A spatial plot of Hg^0/TGM distribution along the cruise track was generated using Ocean Data View (v. 3.0, Reiner Schlitzer, Alfred Wegener Institute for Polar and Marine Research, Bremerhaven, Germany).

3 Results and discussion

3.1 General observations

The time series of the concentrations of the trace gases TGM/Hg^0, CO and O_3 in ambient air samples is shown in Fig. 2. Periods with passage through sea ice are indicated by the blue shading. The spatial distribution of Hg^0/TGM is included in Fig. 1. The time series for RGM and PHg during the polar transect is separately displayed in Fig. 3. An absolute majority of the recorded PHg concentrations were below MDL, whereas the corresponding fraction for RGM was at 50%. The air samples generally comprised the pristine marine boundary layer (MBL), however, it also include several episodes of local and regional pollution, which has to be taken into consideration.

3.1.1 Pollution from internal combustion

The local pollution derived from the plume of the ship's internal combustion engine. The NO_x- and CO-containing plume titrates O_3 by thermal oxidation of NO (cf. Eq. 1). Hence, when sampling the ship's plume, the CO/O_3-ratio increased significantly (from between 2 and 8 in background air to between 15 and a few hundreds). The sampling artefact occurred concomitantly with wind direction within a sector of $180\pm60^\circ$ relative to the ship's bow or with wind speeds less than $3\,\mathrm{m\,s^{-1}}$. The conceivable impact of the plume on the Hg^0-levels measured was examined. For events with CO to O_3 ratios larger than 15, the corresponding Hg^0/TGM data was plotted vs. CO (see Fig. 4).

These parameters were only weakly correlated with no obvious trend. This was also the case for PHg and RGM. Hence, we conclude that the exhaust of the IB Oden does not affect the measurements of the mercury components. During the polar transect, IB Oden navigated in tandem with US-CGC Healy (WAGB-20). Occasionally, the plume from US-CGC Healy was intercepting the sampling intakes, likewise without indicating enhanced mercury levels.

In summary, the screening criteria finally used to reject CO and O_3 data possibly influenced by local pollution are: $[CO]/[O_3]>15$, $[CO]>130$ ppbv and $[O_3]<8$ ppbv. A particular air pollution event on 5 August occasioned by an approaching bunker ship in open sea provided an elevated signal of Hg^0/TGM. In this single case, Hg data were screened out. In Fig. 2, these screened data can be distinguished as open symbols (circles, diamonds and squares, respectively).

3.1.2 Regional pollution

Pollution episodes were encountered in a port and along the coast of the Chukchi Peninsula. These events are characterised by elevated TGM and CO mixing ratios at mid-to-low O_3 concentrations (10–15 ppbv). Analysis of back trajectories demonstrated that the air masses previously passed over the Chukchi Peninsula (Sect. 5, See Fig. 1).

3.2 Observations of Arctic and North Atlantic background air

After removing data possibly influenced by internal combustion pollution, Table 2 was constructed showing the descriptive statistics of the measurements. The major trace gas data applying to merely the Arctic Ocean are summarized in Table 3. These sampled parameters have furthermore been divided into observations made over sea ice as well as into monthly information. Since the measurements were made during an extended period on a mobile platform covering major parts of the Arctic, they can be influenced by seasonal as well as spatial concentrations patterns.

Before entering the Canadian Arctic (Labrador Sea into Baffin Bay) measurements represent conditions in the North Atlantic. Accordingly, O_3 mixing ratios between 30 and almost 50 ppbv were observed. In the Canadian Arctic, the airflow shifted from Sect. 1 to 2 leading to a decrease of O_3 to around 15 to 20 ppbv. The drop in ambient O_3 levels may indicate air masses from remote, low-NO_x-environments where more ozone destruction than ozone production occurs during summertime (Helmig et al., 2007). Henceforward, a steady increase in O_3 from 20 to 30 ppbv was observed during the 1-month long polar transect from the Beaufort Sea to the Barents Sea. Trajectory simulations indicated that air masses were advected from long fetches predominantly within the Canadian and Siberian parts of Sect. 3 and sometimes extending into Sect. 5. Besides these trends in the background O_3 concentrations, the time series also indicates numerous short term reductions of O_3, when the mixing ratios dropped to 10 to 15 ppbv.

Compared to O_3 the variability in the CO mixing ratios was smaller. The average values ranged from around 80 ppbv during the first half of the cruise. During the second half of the expedition, we observed a statistically significant (>95% confidence) linear increase in the CO data (slope: 0.3 ppbv day^{-1}, $R=0.50$), until the values reached an average of around 110 ppbv during the second half of September. Nevertheless, even CO mixing ratios showed a short-term variability in the order of several tens of ppbv.

To distinguish between spatial and seasonal trends, Fig. 5 shows the ship-borne data together with measurements performed at the arctic coastal stations Alert and Barrow (Fig. 1) during the same period. Obviously, several of the trends in O_3 and CO concentrations are observed at the coastal stations as well as onboard. This concerns for example the relatively low values for O_3 and CO in July and August and the subsequent increase beginning in the second half of August. We conclude that the observed seasonal cycles of O_3 as well as CO are not restricted to the coastal sites, but also exist over the Arctic Ocean. Therefore, we suggest that the observations at arctic coastal stations regarding O_3 and CO between July and September can be considered as representative for the entire Arctic. Such a homogeneous distribution is also in good agreement with the relatively long chemical lifetimes of O_3 and CO (between weeks and months, Helmig et al., 2007; Novelli et al., 1998) compared to average transport times into the Arctic of several days in summertime (Stohl, 2006).

The largest discrepancies between the arctic coastal stations and the ship borne measurements in the long-term trends were observed for O_3 at the beginning of the cruise. This clearly indicates the influence of the North Atlantic air masses during this part of the cruise, which contribute to elevated O_3 mixing ratios compared to the Arctic. Interestingly, these air masses have no effect on the CO mixing ratios, which appear not to be inferior over the Arctic Ocean compared to the North Atlantic.

The short-term variability in O_3 and CO as observed in the ship borne measurements were in the case of O_3 also apparent at the coastal stations. They might be to some extent obscured in the coastal CO data due to the longer averaging into 1-h averages compared to the 10 min averages collected onboard. Nevertheless, these short-term fluctuations are probably related to pollution events caused by continental sources (Novelli et al., 1998). It is interesting to note, that such pollution events were also observed in the second half of the cruise over the Arctic Ocean at relatively long distances from potential continental sources (Fig. 1).

In Table 2, the RGM and PHg data tabulated include the observations below MDL. Replacing the values below MDL with a constant value of MDL/2 does not influence the overall statistics. By comparison with summer observations (July–September) from Alert, 1995–2002, Oden Hg^0/TGM data exhibit an equivalent statistical median ($1.67\,ng\,m^{-3}$) (Steffen et al., 2005). Analogous to Alert summer data, the magnitude of and variability in the Arctic MBL Hg^0/TGM concentrations were largest during the early phase of the season (Table 3). In a modelling study of bidirectional surface exchange in the Arctic, Dastoor et al. (2008) predicted that only in July a net re-emission of mercury prevails (averaged for years 2002–2004). In Table 3, the observed average Hg^0/TGM concentration has been binned into measurements over open sea and over sea ice (partial and total coverage), respectively. The mean concentration of the first classification ($1.55\pm0.21\,ng\,m^{-3}$) was lower than that of the second ($1.81\pm0.43\,ng\,m^{-3}$). Also apparent in Table 3 is that no significant divergent distribution between ice and open water was observed for either O_3 or CO. This agrees with the homogeneous distribution of both compounds between the Arctic Ocean and the coastal stations, which is mainly governed by large-scale transport and chemical processing in the atmosphere. However, concerning the corresponding DGM data, there was a more striking difference between the averages of the two data bins. Elevated DGM concentrations observed in the surface water of the Arctic Ocean compared to adjacent oceans is presumably due to input by springtime MDEs and large riverine inputs of Hg and DOC as well as limited gas exchange with air due to the sea ice cover (Andersson et al., 2008b). Poulain et al. (2007a) demonstrated the continuous presence of active, cold resistant Hg-reducing microbes in the Arctic Ocean, which do not depend on light. Based on relatively flat vertical profiles of Hg-tot from the Beaufort Sea and the Canadian Archipelago during summer, Outridge et al. (2008) suggested relative minor input from the atmosphere to the Arctic Ocean. St. Louis et al. (2007) reported high levels of DGM ($129\pm36\,\mathrm{ng\,m^{-3}}$) and organo-mercurials in the surface waters near the Ellesmere Island during late spring. Trajectory analysis for Hg^0 measurements at Zeppelin station during 2000–2008 indicates that the Arctic Ocean acts a source of Hg^0 to the atmosphere in July and August (Hirdman et al., 2009). Our Hg^0/TGM data set compares well with that of Aspmo et al. (2006) concerning higher Hg^0/TGM concentrations over ice covered areas. The study by Aspmo et al. (2006) covering northern latitudes 54–85° in summer also included measurements of airborne oxidised mercury (RGM and PHg). Jointly, low concentrations of RGM and PHg were measured.

In Fig. 6, the diurnal variability of CO, O_3 and TGM/Hg^0 mixing ratios are shown in terms of box plots. The day length during air sampling was at least 22 h. In fact, more than 90% of the data was obtained during mid-night sun. No overall distinct diurnal pattern is discernible for either CO, O_3, TGM/Hg^0 or the transient mercury fractions RGM and PHg (not displayed). In general, diurnal cycles of O_3 are small in polar regions (amplitude range 0–1.5 ppbv) and expected to decline with increasing latitude (Helmig et al., 2007). In contrast, during five consecutive days of the initial Atlantic transect diurnal features were observed for TGM (cf. Figs. 1 and 2). Such diurnal variations in TGM have previously been reported from ship-based measurements in more temperate latitudes of the Northern Hemisphere and explained to a large extent be accounted by Hg^0 evasion from surface water (Laurier et al., 2003). Strongly modulated features in TGM/Hg^0 were in the present study, however, above all confined to events with elevated DGM or regional pollution events from the Chukchi Peninsula. The former episodes of considerable interest for this study will be further investigated and discussed below.

3.2.1 The role of air-sea exchange of Hg^0 in the measured atmospheric Hg^0/TGM concentrations

Table 4 shows the correlation matrix for the major trace gases measured including the dissolved gaseous mercury (DGM) in the surface water (Andersson et al., 2008b). All parameters were found to be only weakly inter-correlated. Furthermore, lagged cross-correlation analysis was applied on the subsets of the Hg^0/TGM-DGM data involving periods of a high variability in both variables with high supersaturation of Hg^0 in the sea (such as the passage through certain parts of the Canadian archipelago, the discharge zone of Mackenzie river and the Arctic Ocean at ∼86° N, cf. Fig. 7). By moving Hg^0/TGM towards increasing time domain (typically 2–3 h), a significant improvement in the correlation from overall $R=-0.035$ to $R\sim0.4–0.6$ was obtained for several periods. In Fig. 7, the Hg^0/TGM-DGM data are plotted together with time lags of 2 and 2.5 h for two episodes from different legs of the expedition. The physical rationale for a time delay in the Hg^0/TGM signal is mass transport limitation in the sea-air transfer of the ensued strong supersaturation of DGM (the degree of supersaturation of DGM in the surface sea water (%) can be calculated according to: $S=(\mathrm{DGM}\times k_H/\mathrm{TGM}-1)\times100$, where k_H is the dimensionless Henry's law constant determined e.g. by Andersson et al., 2008a). For a sparingly soluble gas like Hg^0(g) the hydrodynamic barrier delaying the increasing DGM levels to be propagated into the air. The cases presented refer to a partially open sea (Fig. 7a) and an icebound sea (Fig. 7b). In the ice-covered oceanic surface waters such as in Fig. 7b, it is likely that elevated DGM concentrations were built up due to the restricted air exchange (Andersson et al., 2008b). On the other hand, the formation rate of DGM is dependant on biotic and abiotic reduction of Hg^{II}(aq) and a cap of sea-ice will attenuate photoreduction and retard DGM formation. The headway of IB Oden including the ice breaking presumably influences the gas-exchange of Hg^0 positively.

The future predictions for the cycling of mercury in the Arctic are coupled with changes in the climate system. The global warming has and will have a profound and extensive impact on the biogeochemical cycle of Hg in the polar regions. The minimum sea-ice extent of the Arctic Ocean has decreased at an average of (−7.4±2.4) % per decade since 1979 while the corresponding decrease of mean annual extent of Arctic sea-ice is only at (−2.7±0.6) % per decade (Lemke et al., 2007). Simulations indicate abrupt future reduction reaching near ice-free September conditions by 2040 (Holland et al., 2006). As climate warming presumably will initially influence the magnitude and spatial extent of Arctic MDEs and boost photo-reduction of Hg^{II}(aq) the efflux of Hg^0 from the Arctic Ocean to the atmosphere during summer is predicted to rapidly increase in the near future. Using a model developed by Nightingale et al. (2000), Andersson et al. (2008b) calculated a hypothetical average Hg^0 evasion of ∼60 ng m^{-2} day^{-1} during the Beringia 2005 expedition with a maximum as high as ∼2300 ng m^{-2} day^{-1}. St. Louis et al. (2007) calculated a Hg^0 flux of 130±30 ng m^{-2} day^{-1} at ice break-up. In-turn Outridge et al. (2008) predict a 8-fold increase in summer Hg^0 flux for the future between 60° N and 80–90° N. The average Hg turnover time for the upper Arctic Ocean, which is at present ∼5 years, may thus decrease.

3.2.2 The oxidation capacity of the Arctic MBL during summer

The low O_3 concentrations in July and August agree well with the analysis of air mass transport from the Arctic Ocean to a coastal site in the Arctic (Hirdman et al., 2009). The detailed trajectory analysis for O_3 measurements at Zeppelin station indicates that the Arctic Ocean constitutes a sink for O_3 in spring- and summertime. While the destruction of O_3 in April and May is related to ozone depletion events (ODEs) leading to the complete removal of O_3 in the MBL (Simpson et al., 2007), the lower O_3 concentrations in summer may be due to a combination of processes. The chemical destruction of O_3 as a result of halogen activation from the abundant sea salt can continue, although it is necessarily less effective than in springtime since no ODEs have yet been observed in summer (Simpson et al., 2007). The low NO_x-environment like the Arctic can also contribute to a more efficient chemical O_3 destruction during summer (Helmig et al., 2007). Both processes are related to the levels of incoming solar radiation, which start to decrease in late summer in the high latitudes. In addition, a more effective deposition to the open water areas compared to the snow-covered sea ice can reduce the O_3 concentrations in the MBL (e.g. Gallagher et al., 2001; Helmig et al. 2009). In contrast, the absence of any significant diurnal variability for O_3 indicates that in situ photochemical production in the Arctic MBL is low during this period of time.

In the case of CO, the summertime minimum can be attributed to the removal of CO by the reaction with hydroxyl radicals (Novelli et al., 1998); which is also more efficient during summer compared to the fall.

The measurement of airborne Hg^0, RGM and PHg during the Polar transect of leg 3 indicates that the Arctic Ocean MBL during summer does not promote significant chemical conversion of Hg^0 and consequently constitutes a minor source of RGM and PHg. The speciated-Hg observations are in concert with those of Temme et al. (2003) and Aspmo et al. (2006) for the South Atlantic and the North Atlantic/Arctic Ocean, respectively during Polar summer. Observations at mid-latitudes indicate that the oxidising capacity of the MBL enriched with halide-abundant aerosols induces a significant Hg^0 loss (Mason et al., 2003). However, the MBL of the Arctic Ocean during summer is distinguished by meteorological factors (high relative humidity, low visibility blocking solar radiation) not in favour of in-situ oxidation and in promotion of physical scavenging and removal of RGM and PHg. For example, leg 3 was characterised by frequent fogs and a median relative humidity of 93%.

4 Conclusions

For first time we were able to perform measurements of airborne speciated-Hg together with O_3 and CO over major parts of the Arctic Ocean and adjacent seas during the polar summer period. The prevalent conditions of the Arctic MBL during the expedition resulted in relatively narrow statistical distributions of the trace gases (especially for CO). The largest relative variability was present in the Hg^0/TGM data set during July, where generally higher concentrations were measured over the ice-capped sea. The results presented in this paper suggest the Arctic Ocean during summer to be a significant source of Hg^0 to the atmosphere. ODEs and MDEs, which occur regularly during polar spring, where not observed and, therefore, do not contribute to the removal of mercury and O_3 during summer. This agrees well with the seasonal cycle of BrO in high latitudes derived from remote sensing data (Hollwedel et al., 2004). BrO is one of the intermediate species generated during the ODEs and hence can be used as an indicator for such events. Nevertheless, O_3 values lower than in the background air of the North Atlantic indicate an ongoing removal of O_3 from the Arctic MBL in summer probably due to a combination of chemical and physical processes. The good agreement between the ship-borne measurements of O_3 and CO and the observations at Barrow and Alert indicate that the observed seasonal variation between July and September are representative for the entire Arctic. In terms of an abrupt future warming, the current cycling of Hg in the Arctic will be largely perturbed and sea-air interaction will be even more important in its atmospheric behaviour.

Acknowledgements. The Swedish Polar Secretariat is acknowledged for organising and including our project in the BERINGIA 2005 expedition. The Captain and crew of IB Oden are greatly appreciated for the support and help onboard. Special thanks go to C. Temme (previously at G.K.S.S. Research Centre, Geesthacht, Germany) for kindly providing an analytical instrument for the expedition. The authors thank P. Novelli (NOAA/ESRL) and the Air Quality Research Division of Environment Canada for providing unpublished data from Barrow and Alert and the Japan Meteorological Agency for maintaining the WMO World Data Centre for Greenhouse Gases. The authors gratefully acknowledge the NOAA Air Resources Laboratory

(ARL) for the provision of the HYSPLIT transport and dispersion model and READY website (www.arl.noaa.gov/ready.html) used in this publication. This research was partly supported by grants from the German Academic Exchange Service (DAAD) and the Swedish Foundation for International Cooperation in Research and Higher Education (STINT).

References

Andersson, M. E.: Transport of Mercury Species in the Environment – Exchange Between Oceanic Waters and the Atmosphere, Ph.D. thesis, Department of Chemistry, Göteborg University, Sweden, 59 pp., 2008.

Andersson, M. E.: Concentrations and distribution of speciated mercury in the Arctic Ocean, unpublished manuscript.

Andersson, M. E., Gårdfeldt, K., Wängberg, I., and Strömberg, D.: Determination of Henry's law constant for elemental mercury, Chemosphere, 73, 587–592, 2008a.

Andersson, M. E., Sommar, J., Gårdfeldt, K., and Lindqvist, O.: Enhanced concentrations of dissolved gaseous mercury in the surface waters of the Arctic Ocean, Mar. Chem., 110, 190–194, 2008b.

Ariya, P. A., Dastoor, A. P., Amyot, M., Schroeder, W. H., Barrie, L., Anlauf, K., Raofie, F., Ryzhkov, A., Davignon, D., Lalonde, J., and Steffen, A.: The Arctic: A sink for mercury, Tellus B, 56, 397–403, 2004.

Aspmo, K., Temme, C., Berg, T., Ferrari, C., Gauchard, P.-A., Fain, X., and Wibetoe, G.: Mercury in the atmosphere, snow and melt water ponds in the North Atlantic Ocean during Arctic summer, Environ. Sci. Technol., 40, 4083–4089, 2006.

Banic, C. M., Beauchamp, S. T., Tordon, R. J., Schroeder, W. H., Steffen, A., Anlauf, K. A., and Wong, H. K. T.: Vertical distribution of gaseous elemental mercury in Canada, J. Geophys. Res.-Atmos., 108, 4264, doi:10.1029/2002JD002116, 2003.

Berg, T., Sekkesæter, S., Steinnes, E., Valdal, A.-K., and Wibetoe, G.: Arctic springtime depletion of mercury in the European Arctic as observed at Svalbard, Sci. Total Environ., 304, 43–51, 2003.

Brooks, S. B., Saiz-Lopez, A., Skov, H., Lindberg, S. E., Plane, J. M. C., and Goodsite, M. E.: The mass balance of mercury in the springtime Arctic environment, Geophys. Res. Lett., 33, LI3812, doi:10.1029/2005GL025525, 2006.

Calvert, J. G. and Lindberg, S. E.: Mechanisms of mercury removal by O_3 and OH in the atmosphere, Atmos. Environ., 39, 3355–3367, 2005.

Dastoor, A. P., Davignon, D., Theys, N., Van Roozendael, M., Steffen, A., and Ariya, P. A.: Modeling dynamic exchange of gaseous elemental mercury at polar sunrise, Environ. Sci. Technol., 42, 5183–5188, 2008.

Donohoue, D. L., Bauer, D., Cossairt, B., and Hynes, A. J.: Temperature and pressure dependent rate coefficients for the reaction of Hg with Br and the reaction of Br with Br: A pulsed laser photolysis–pulsed laser induced fluorescence study, J. Phys. Chem. A, 110, 6623–6632, 2006.

Draxler, R. R. and Rolph, G. D.: HYSPLIT (HYbrid Single-Particle Lagrangian Integrated Trajectory) model access via NOAA ARL READY website (http://www.arl.noaa.gov/ready/hysplit4.html), NOAA Air Resources Laboratory, Silver Spring, MD, 2003.

Ebinghaus, R., Kock, H. H., Temme, C., Einax, J. W., Löwe, A. G., Richter, A., Burrows, J. P., and Schroeder, W. H.: Antarctic springtime depletion of atmospheric mercury, Environ. Sci. Technol., 36, 1238–1244, 2002.

Ebinghaus, R., Slemr, F., Brenninkmeijer, C. A. M., van Velthoven, P., Zahn, A., Hermann, M., O'Sullivan, D. A., and Oram, D. E.: Emissions of gaseous mercury from biomass burning in South America in 2005 observed during CARIBIC flights, Geophys. Res. Lett., 34, L08813, doi:10.1029/2006GL028866, 2007.

Eneroth, K., Holmén, K., Berg, T., Schmidbauer, N., and Solberg, S.: Springtime depletion of tropospheric ozone, gaseous elemental mercury and non-methane hydrocarbons in the European Arctic, and its relation to atmospheric transport, Atmos. Environ., 41, 8511–8526, 2007.

Gallagher, M. W., Beswick, K. M., and Coe, H.: Ozone deposition to coastal waters, Q. J. Roy. Meteor. Soc., 127, 539–558, 2001.

Gerbig, C., Schmitgen, S., Kley, D., Volz-Thomas, A., Dewey, K., and Haaks, D.: An improved fast-response vacuum-UV resonance fluorescence CO instrument, J. Geophys. Res.-Atmos., 104, 1699–1704, 1999.

Hedgecock, I. M., Pirrone, N., and Sprovieri, F.: Chasing quicksilver northward: Mercury chemistry in the Arctic troposphere, Environ. Chem., 5, 131–134, 2008.

Helmig, D., Oltmans, S. J., Carlson, D., Lamarque, J.-F., Jones, A., Labuschagne, C., Anlauf, K., and Hayden, K.: A review of surface ozone in the polar regions, Atmos. Environ., 41, 5138–5161, 2007.

Helmig, D., Cohen, L. D., Bocquet, F., Oltmans, S., Grachev, A., and Neff, W.: Spring and summertime diurnal surface ozone fluxes over the polar snow at Summit, Greenland, Geophys. Res. Lett., 36, L08809, doi:10.1029/2008GL036549, 2009.

Hirdman, D., Aspmo, C., Burkhart, J. F., Eckhardt, S., Sodemann, H., and Stohl, A.: Transport of mercury in the Arctic atmosphere: Evidence for a spring-time net sink and summer-time source, Geophys. Res. Lett., 36, L12814, doi:10.1029/2009GL038345, 2009.

Holland, M. M., Bitz, C. M., and Tremblay, B.: Future abrupt reductions in the summer Arctic sea ice, Geophys. Res. Lett., 33, L23503, doi:10.1029/2006GL028024, 2006.

Holloway, T., Levy II, H., and Kasibhatla, P.: Global distribution of carbon monoxide, J. Geophys. Res., 105, 12123–12147, 2000.

Hollwedel, J., Wenig, M., Beirle, S., Kraus, S., Kuhl, S., Wilms-Grabe, W., Platt, U., and Wagner, T.: Year-to-year variations of spring time polar tropospheric BrO as seen by GOME, Adv. Space Res., 34, 804–808, doi:10.1016/j.asr.2003.08.060, 2004.

Hönninger, G.: Halogen Oxide Studies in the Boundary Layer by Multi Axis Differential Optical Absorption Spectroscopy and Active Longpath-DOAS., Ph.D. thesis, Institute of Environmental Physics, University of Heidelberg, Germany, 262 pp., 2002.

IHO: Limits of Oceans and Seas, Special Publication 23, International Hydrographic Organization, Monaco, 1953.

Jacobi, H. W. and Schrems, O.: Peroxyacetyl nitrate (PAN) distribution over the South Atlantic Ocean, Phys. Chem. Chem. Phys., 1, 5517–5521, 1999.

Jacobi, H. W., Kaleschke, L., Richter, A., Rozanov, A., and Burrows, J. P.: Observation of a fast ozone loss in the marginal ice zone of the Arctic Ocean, J. Geophys. Res.-Atmos., 111, D15309, doi:10.1029/2005JD006715, 2006.

Jaffe, D., Prestbo, E., Swartzendruber, P., Weiss-Penzias, P., Kato, S., Takami, A., Hatakeyama, S., and Kajii, Y.: Export of atmospheric mercury from Asia, Atmos. Environ., 39, 3029–3038, 2005.

Kaleschke, L., Richter, A., Burrows, J., Afe, O., Heygster, G., Notholt, J., Rankin, A. M., Roscoe, H. K., Hollwedel, J., Wagner, T., and Jacobi, H. W.: Frost flowers on sea ice as a source of sea salt and their influence on tropospheric halogen chemistry, Geophys. Res. Lett., 31, L16114, doi:10.1029/2004GL020655, 2004.

Kellerhals, M., Beauchamp, S., Belzer, W., Blanchard, P., Froude, F., Harvey, B., McDonald, K., Pilote, M., Poissant, L., Puckett, K., Schroeder, B., Steffen, A., and Tordon, R.: Temporal and spatial variability of total gaseous mercury in Canada: Results from the Canadian Atmospheric Mercury Measurement Network (CAMNet), Atmos. Environ., 37, 1003–1011, 2003.

Kim, K. H., Ebinghaus, R., Schroeder, W. H., Blanchard, P., Kock, H. H., Steffen, A., Froude, F. A., Kim, M. Y., Hong, S. M., and Kim, J. H.: Atmospheric mercury concentrations from several observatory sites in the Northern Hemisphere, J. Atmos. Chem., 50, 1–24, 2005.

Kock, H. H., Bieber, E., Ebinghaus, R., Spain, T. G., and Thees, B.: Comparison of long-term trends and seasonal variations of atmospheric mercury concentrations at the two European coastal monitoring stations Mace Head, Ireland, and Zingst, Germany, Atmos. Environ., 39, 7549–7556, 2005.

Lahoutifard, N., Poissant, L., and Scott, S. L.: Scavenging of gaseous mercury by acidic snow at Kuujjuarapik, Northern Quebec, Sci. Total Environ., 355, 118–126, 2006.

Laurier, F. J. G., Mason, R. P., Whalin, L., and Kato, S.: Reactive gaseous mercury formation in the North Pacific Ocean's marine boundary layer: A potential role of halogen chemistry, J. Geophys. Res.-Atmos., 108, L16114, doi:10.1029/2003JD003625, 2003.

Lemke, P., J. Ren, R. B. Alley, I. Allison, J. Carrasco, G. Flato, Y. Fujii, G. Kaser, P. Mote, R. H. Thomas, and Zhang, T.: Observations: Changes in Snow, Ice and Frozen Ground, in: Climate Change 2007: The Physical Science Basis. Contribution of Working Group I to the Fourth Assessment Report of the Intergovernmental Panel on Climate Change, edited by: Solomon, S., Qin, D., Manning, M., Chen, Z., Marquis, M., Averyt, K. B., Tignor, M. and Miller, H. L., Cambridge University Press, Cambridge, UK and New York, NY, USA, 2007.

Lockhart, W. L., Stern, G. A., Wagemann, R., Hunt, R. V., Metner, D. A., DeLaronde, J., Dunn, B., Stewart, R. E. A., Hyatt, C. K., Harwood, L., and Mount, K.: Concentrations of mercury in tissues of beluga whales (Delphinapterus leucas) from several communities in the Canadian Arctic from 1981 to 2002, Sci. Total Environ., 351, 391–412, 2005.

Mason, R. P., Laurier, F. J. G., Whalin, L., and Sheu, G. R.: The role of ocean-atmosphere exchange in the global mercury cycle, J. Phys. IV, 107, 835–838, 2003.

Nightingale, P. D., Malin, G., Law, C. S., Watson, A. J., Liss, P. S., Liddicoat, M. I., Boutin, J., and Upstill-Goddard, R. C.: In situ evaluation of air-sea gas exchange parameterizations using novel conservative and volatile tracers, Global Biogeochem. Cy., 14, 373–387, 2000.

Novelli, P. C., Masarie, K. A., and Lang, P. M.: Distributions and recent changes of carbon monoxide in the lower troposphere, J. Geophys. Res.-Atmos., 103, 19015–19033, 1998.

Obrist, D.: Atmospheric mercury pollution due to losses of terrestrial carbon pools?, Biogeochemistry, 85, 119–123, 2007.

Outridge, P. M., Macdonald, R. W., Wang, F., Stern, G. A., and Dastoor, A. P.: A mass balance inventory of mercury in the Arctic Ocean, Environ. Chem., 5, 89–111, 2008.

Poulain, A. J., Chadhain, S. M. N., Ariya, P. A., Amyot, M., Garcia, E., Campbell, P. G. C., Zylstra, G. J., and Barkay, T.: Potential for mercury reduction by microbes in the high Arctic, Appl. Environ. Microb., 73, 2230–2238, 2007a.

Poulain, A. J., Garcia, E., Amyot, M., Campbell, P. G. C., and Ariya, P. A.: Mercury distribution, partitioning and speciation in coastal vs. inland High Arctic snow, Geochim. Cosmochim. Ac., 71, 3419–3431, 2007b.

Schroeder, W. H., Anlauf, K. G., Barrie, L. A., Lu, J. Y., Steffen, A., Schneeberger, D. R., and Berg, T.: Arctic springtime depletion of mercury, Nature, 394, 331–332, 1998.

Schroeder, W. H., Steffen, A., Scott, K., Bender, T., Prestbo, E., Ebinghaus, R., Lu, J. Y., and Lindberg, S. E.: Summary report: First international Arctic atmospheric mercury research workshop, Atmos. Environ., 37, 2551–2555, 2003.

Sigler, J. M., Lee, X., and Munger, W.: Emission and long-range transport of gaseous mercury from a large-scale Canadian boreal forest fire, Environ. Sci. Technol., 37, 4343–4347, 2003.

Simpson, W., Alvarez-Avilies, L., Douglas, T. A., Sturm, M., and Domine, F.: Halogens in the coastal snow pack near Barrow, Alaska: Evidence for active bromine air-snow chemistry during springtime, Geophys. Res. Lett., 32, L04811, doi:10.1029/2004GL021748, 2005.

Simpson, W. R., von Glasow, R., Riedel, K., Anderson, P., Ariya, P., Bottenheim, J., Burrows, J., Carpenter, L. J., Frieß, U., Goodsite, M. E., Heard, D., Hutterli, M., Jacobi, H.-W., Kaleschke, L., Neff, B., Plane, J., Platt, U., Richter, A., Roscoe, H., Sander, R., Shepson, P., Sodeau, J., Steffen, A., Wagner, T., and Wolff, E.: Halogens and their role in polar boundary-layer ozone depletion, Atmos. Chem. Phys., 7, 4375–4418, 2007, http://www.atmos-chem-phys.net/7/4375/2007/.

Skov, H., Christensen, J. H., Goodsite, M. E., Heidam, N. Z., Jensen, B., Wåhlin, P., and Geernaert, G.: Fate of elemental mercury in the Arctic during atmospheric mercury depletion episodes and the load of atmospheric mercury to the Arctic, Environ. Sci. Technol., 54, 2373–2382, 2004.

Slemr, F., Schuster, G., and Seiler, W.: Distribution, speciation, and budget of atmospheric mercury, J. Atmos. Chem., 3, 407–434, 1985.

Slemr, F., Ebinghaus, R., Simmonds, P. G., and Jennings, S. G.: European emissions of mercury derived from long-term observations at Mace Head, on the western Irish coast, Atmos. Environ., 40, 6966–6974, 2006.

Slemr, F., Brunke, E. G., Labuschagne, C., and Ebinghaus, R.: Total gaseous mercury concentrations at the Cape Point GAW station and their seasonality, Geophys. Res. Lett., 35, L11807, doi:10.1029/2008GL033741, 2008.

Sommar, J., Hallquist, M., Ljungström, E., and Lindqvist, O.: On the gas phase reactions between volatile biogenic mercury species and the nitrate radical, J. Atmos. Chem., 27, 233–247, 1997.

Sommar, J., Gårdfeldt, K., Strömberg, D., and Feng, X. B.: A kinetic study of the gas-phase reaction between the hydroxyl radical and atomic mercury, Atmos. Environ., 35, 3049–3054, 2001.

Sommar, J., Wängberg, I., Berg, T., Gårdfeldt, K., Munthe, J., Richter, A., Urba, A., Wittrock, F., and Schroeder, W. H.: Circumpolar transport and air-surface exchange of atmospheric mercury at Ny-Ålesund (79° N), Svalbard, spring 2002, Atmos. Chem. Phys., 7, 151–166, 2007, http://www.atmos-chem-phys.net/7/151/2007/.

St. Louis, V. L., Hintelmann, H., Graydon, J. A., Kirk, J. L., Barker, J., Dimock, B., Sharp, M. J., and Lehnherr, I.: Methylated mercury species in Canadian high arctic marine surface waters and snowpacks, Environ. Sci. Technol., 41, 6433–6441, 2007.

Steffen, A., Schroeder, W. H., Macdonald, R. W., Poissant, L., and Konoplev, A.: Mercury in the Arctic atmosphere: An analysis of eight years of measurements of GEM at Alert (Canada) and a comparison with observations at Amderma (Russia) and Kuujjuarapik (Canada). Sci. Total Environ., 342, 185–198, 2005.

Steffen, A., Douglas, T., Amyot, M., Ariya, P., Aspmo, K., Berg, T., Bottenheim, J., Brooks, S., Cobbett, F., Dastoor, A., Dommergue, A., Ebinghaus, R., Ferrari, C., Gårdfeldt, K., Goodsite, M. E., Lean, D., Poulain, A. J., Scherz, C., Skov, H., Sommar, J., and Temme, C.: A synthesis of atmospheric mercury depletion event chemistry in the atmosphere and snow, Atmos. Chem. Phys., 8, 1445–1482, 2008, and references therein.

Stohl, A.: Characteristics of atmospheric transport into the Arctic troposphere, J. Geophys. Res., 111, D11306, doi:10.1029/2005JD006888, 2006.

Stohl, A., Berg, T., Burkhart, J. F., Fjæraa, A. M., Forster, C., Herber, A., Hov, Ø., Lunder, C., McMillan, W. W., Oltmans, S., Shiobara, M., Simpson, D., Solberg, S., Stebel, K., Ström, J., Tørseth, K., Treffeisen, R., Virkkunen, K., and Yttri, K. E.: Arctic smoke– record high air pollution levels in the European Arctic due to agricultural fires in Eastern Europe in spring 2006, Atmos. Chem. Phys., 7, 511–534, 2007, http://www.atmos-chem-phys.net/7/511/2007/.

Sumner, A. L., Shepson, P. B., Grannas, A. M., Bottenheim, J. W., Anlauf, K. G., Worthy, D., Schroeder, W. H., Steffen, A., Domine, F., Perrier, S., and Houdier, S.: Atmospheric chemistry of formaldehyde in the Arctic troposphere at polar sunrise, and the influence of the snowpack, Atmos. Environ., 36, 2553–2562, 2002.

Wängberg, I., Munthe, J., Amouroux, D., Andersson, M. E., Fajon, V., Ferrara, R., Gårdfeldt, K., Horvat, M., Mamane, Y., Melamed, E., Monperrus, M., Ogrinc, N., Yossef, O., Pirrone, N., Sommar, J., and Sprovieri, F.: Atmospheric mercury at Mediterranean coastal stations, Environ. Fluid Mech., 8, 101–116, 2008.

Wilhelm, S. M.: Estimate of mercury emissions to the atmosphere from petroleum, Environ. Sci. Technol., 35, 4704–4710, 2001.

Wängberg, I., Munthe, J., Ebinghaus, R., Gårdfeldt, K., Iverfeldt, Å., and Sommar, J.: Distribution of TPM in Northern Europe, Sci. Total Environ., 304, 53–59, 2003.

Table 1. Information concerning the air sampling protocol onboard IB Oden (4th deck).

Species	Freq.	Start (dd-mm-yy hh:mm)	Stop (dd-mm-yy hh:mm)	Instrument
Hg^0/TGM	12 h^{-1}	05-07-05 14:20	24-09-05 11:00	Tekran 2537A CVAFS[a]
RGM-PHg	4 day^{-1}	25-08-05 16:00	22-09-05 17:00	Front sampler+Tekran 2537A CVAFS
O_3	6 h^{-1}	05-07-05 12:10	22-09-05 12:00	$O_3$41M Ansyco Environnement
CO	120 h^{-1}	06-07-05 10:00	24-09-05 16:20	AL 5001 AeroLaser

[a] Front-sampler used during leg 3.

Table 2. Summary of the measurements after screening the raw data from local combustion.

Species	*N*	Mean	Min	Max	Median	SD	RSD
Hg^0/TGM (ng m^{-3})	9061	1.73	1.00	5.24	1.67	0.36	0.21
DGM (ng m^{-3})	6138	42.4	4.9	207.4	37.7	25.9	0.61
O_3 (ppbv)	9793	21.4	8.0	47.3	21.0	5.5	0.27
CO (ppbv)	10 000	84.4	50.3	223.8	84.0	11.6	0.14
RGM (pg m^{-3})	57	3.2	0.7 (ND)	10.0	3.1	1.7	0.53
PHg (pg m^{-3})	54	1.0	0.2 (ND)	3.2	0.9 (ND)	0.7	0.71

Title Page
Abstract
Introduction
Conclusions
References
Tables
Figures
◀|
|▶
◀
▶
Back
Close
Full Screen / Esc
Printer-friendly Version
Interactive Discussion

Table 3. Summary of screened Hg^0/TGM, O_3 and CO data applicable to the Arctic Ocean (incl. Baffin Bay, Northwest Passages, Beaufort Sea, Chukchi Sea, and Greenland Sea). Excluded are thus data from the North Atlantic Ocean, Labrador Sea and Bering Sea (IHO, 1953).

Species	Overall			July			August			September			Sea Ice			Sea w/o ice		
	N	Mean	SD	*N*	Mean	SD	*N*	Mean	SD	*N*	Mean	SD	*N*	Mean	SD	*N*	Mean	SD
Hg^0/TGM (ng m^{-3})	7864	1.72	0.35	1737	2.08	0.44	3686	1.62	0.24	2441	1.61	0.20	5443	1.81	0.41	2421	1.55	0.21
O_3 (ppbv)	8491	20.6	4.6	2435	17.3	3.1	3859	20.4	3.4	2197	24.5	4.7	5921	21.1	4.8	2570	19.4	3.9
CO (ppbv)	9276	87.0	11.8	2396	80.9	11.2	4060	84.3	9.4	2820	96.2	9.9	6215	87.3	10.4	3061	86.5	14.3

Table 4. Over-all correlation matrix of trace gases and DGM.

Species	Hg^0/TGM	DGM	O_3	CO
Hg^0/TGM	×			
DGM	−0.035	×		
O_3	−0.266	−0.027	×	
CO	−0.086	0.155	0.036	×

Title Page
Abstract Introduction
Conclusions References
Tables Figures
◀▮ ▶▮
◀ ▶
Back Close
Full Screen / Esc
Printer-friendly Version
Interactive Discussion

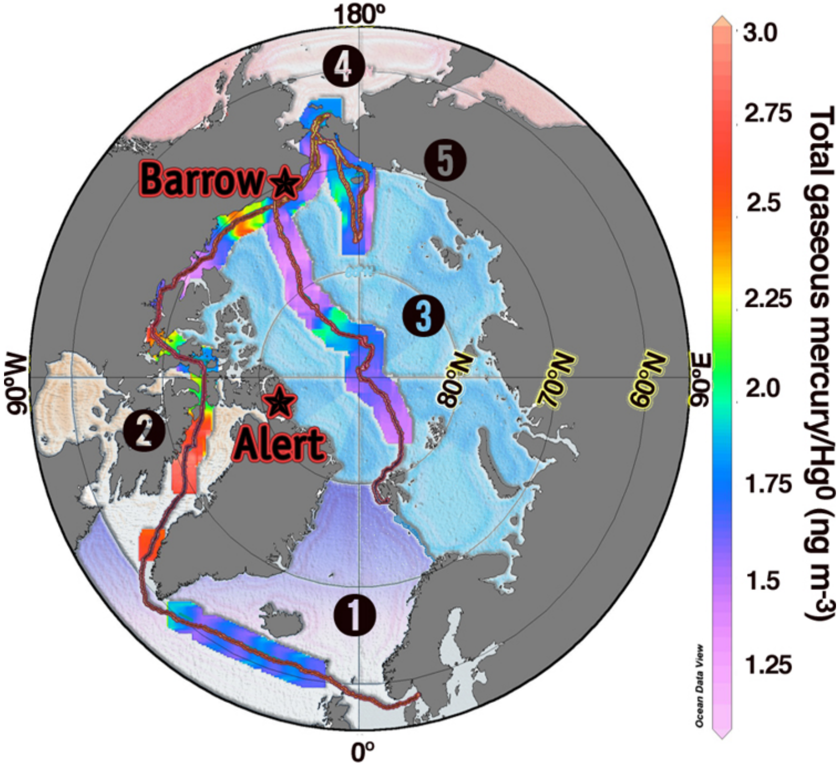

Fig. 1. The spatial distribution of Hg^0/TGM in air (ng m^{-3}) along the cruise track. The map has been divided into five sectors to classify the source region of the five-day back-trajectories arriving at IB Oden: 1) North Atlantic Ocean, 2) Canadian archipelago, 3) Arctic Ocean, 4) North Pacific Ocean and 5) Chukchi Peninsula/Siberia. Also included are the locations of Alert (Nunavut, Canada) and Barrow (Alaska, USA).

ACPD

9, 20913–20948, 2009

Circumpolar measurements in the boundary layer of the Arctic Ocean

J. Sommar et al.

Title Page
Abstract | Introduction
Conclusions | References
Tables | Figures
I◀ | ▶I
◀ | ▶
Back | Close
Full Screen / Esc
Printer-friendly Version
Interactive Discussion

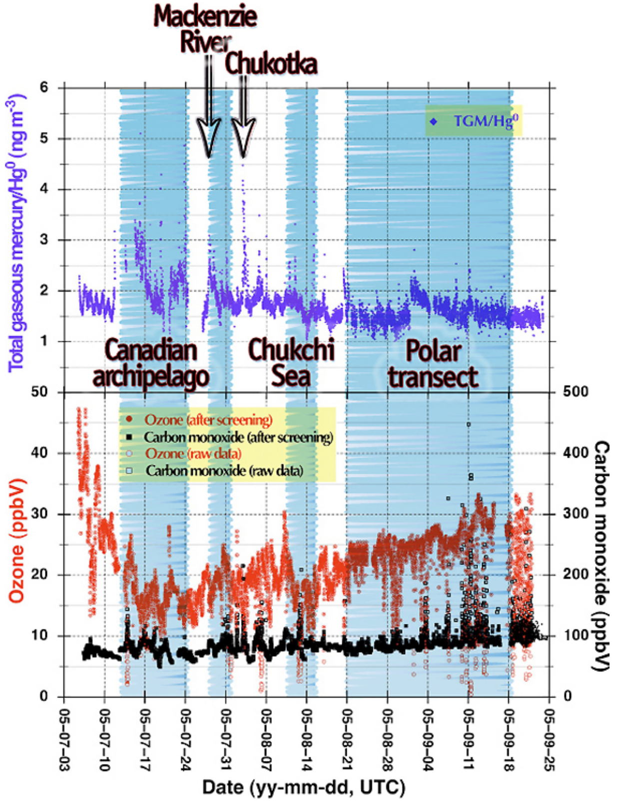

Fig. 2. 10 min averaged concentrations of atmospheric trace gases Hg^0/TGM, O_3, CO over the northern Atlantic and Arctic Ocean measured onboard the IB Oden during BERINGIA 2005. Passage through ice-covered sea is shaded in bluish colours. The names of some important geographical area discernible in Fig. 1 are indicated as well.

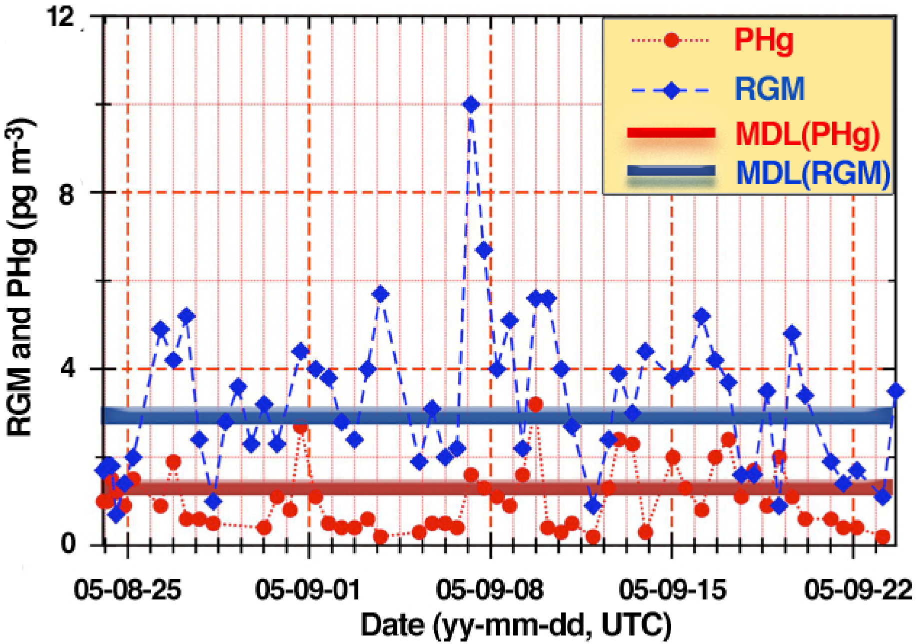

Fig. 3. Concentrations of atmospheric Hg fractions RGM (blue diamonds) and PHg (red circles) measured with a frequency of 4 samples per day along the trans-polar route. Drawing the detection limit for each fraction indicates the sampling data points below MDL.

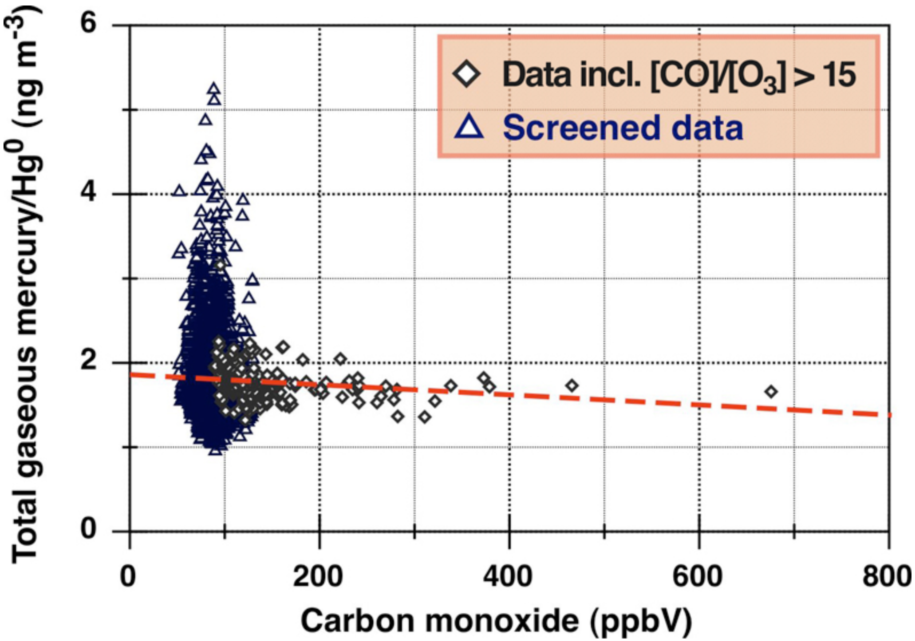

Fig. 4. The relationship between Hg^0/TGM and CO during events of pollution from the ship's internal engine determined by a ratio of CO/O$_3$ larger than 15. Also included are the data screened according to Chap. 3.1.1 but not comprised in the linear regression fit. The parameters are only weakly correlated implying that the ship's emissions are negligible with respect to Hg.

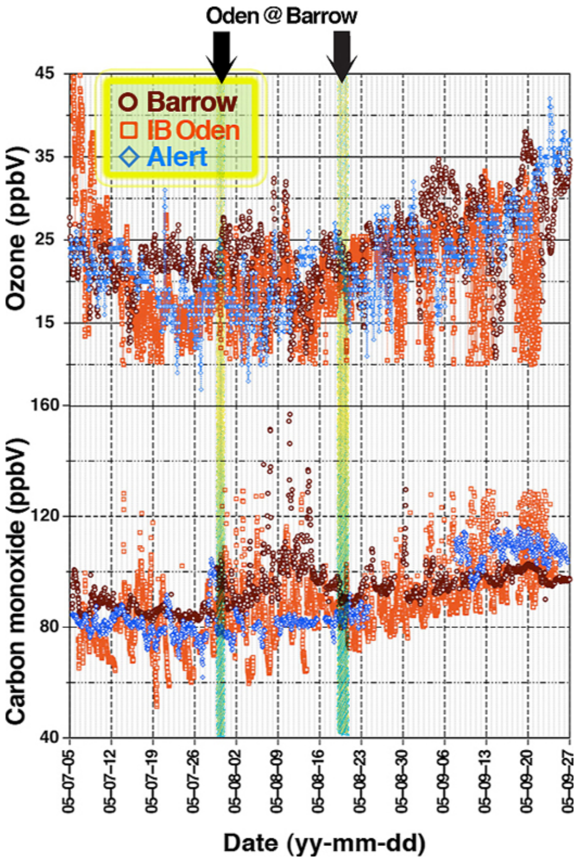

Fig. 5. Comparison of Oden, Barrow and Alert observations for O_3 (upper panel) and for CO (lower panel). The time series from IB Oden are comprised of 10 min averaged data while the others refer to hourly averaged data. Periods shaded in yellow-green resemble anchorage time of IB Oden outside Pt. Barrow.

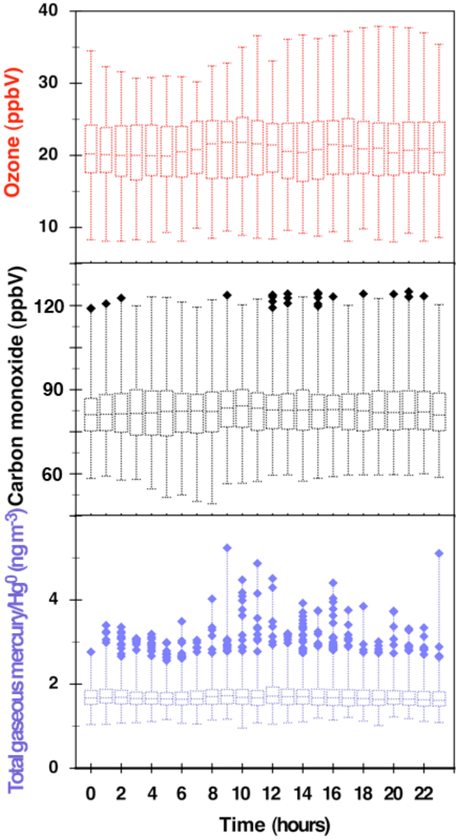

Fig. 6. Diurnal variations of the O_3, CO and Hg^0/TGM concentrations summarised as in Table 2. The box assemblies include the mean, the upper and lower 95% confidence intervals and extremes (far outliers) for 1 h per bin diurnally integrated samples. The UTC time data has been recalculated to represent destination local time.

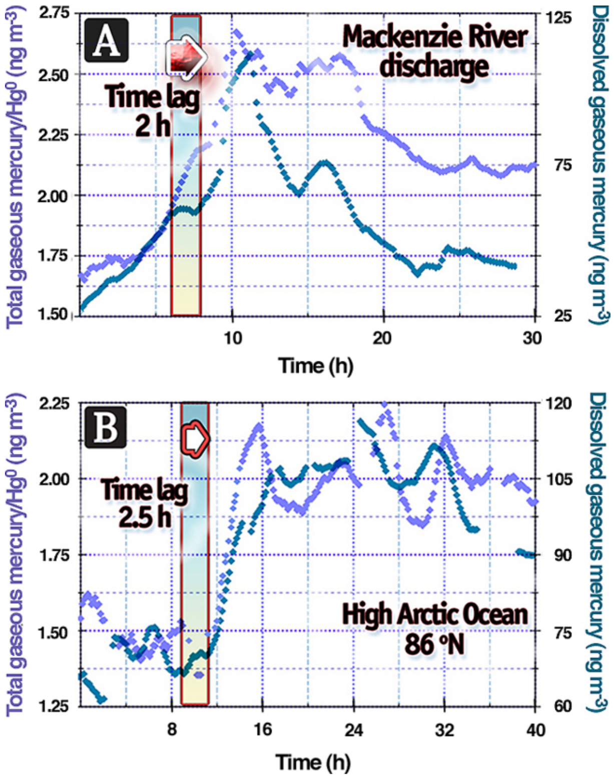

Fig. 7. The temporal air-sea distribution of Hg^0 vapour for two specific destinations: **(a)** Mackenzie River discharge and b) High Arctic Ocean (~86° N). Cross-correlation analysis revealed a maximised Hg^0/TGM-DGM covariance for time lags of 2 h and 2.5 h, respectively. Thus, the time-series of Hg^0/TGM and DGM has been shifted in (a) by 2 h and in **(b)** by 2.5 h. The maximum coefficient of correlation is 0.59 (n=188) in case a and 0.54 (n=307) in case b). The distribution of Hg^0 between air and sea is in both cases in strong disequilibrium.